NFFT: Algorithm for irregular sampling

Akshay Gulati and Robert J. Ferguson

ABSTRACT

The nonuniform discrete Fourier transform (NDFT), used in many processing schemes, can be computed using a fast algorithm known as the non uniform fast Fourier transform (NFFT). The NFFT is not a new algorithm, but it is an approximation scheme that can be use to calculate an approximate spectrum. In one dimension, computational complexity of the NFFT is $O(NlogN)$ which is a dramatic improvement from the $O(N^2)$ complexity of the NDFT. This algorithm can be easily extended to higher dimensions.

The approximate spectrum is calculated using a simple algorithm scheme which involves convolution of an irregularly sampled signal with a truncated Gaussian in the spatial domain. A new empirical expression based on numerical experiment for the analytical Gaussian width is proposed. Synthetic data examples, some with analytical solutions, demonstrate the utility and validity of this approach. The approximate spectrum obtained can be use further in a reconstruction algorithm. This algorithm removes the bottle neck from forward process by replacing NDFT with NFFT in many conventional processing algorithms.

INTRODUCTION

The problem of analyzing a signal $P(t_j)$ having irregularly spaced measurements is common in geophysics (Zwartjes and Sacchi, 2007). Faulty equipment, errors in positioning, obstacles, and noise sources can be reasons for irregularly spaced measurements. Many aspects of conventional seismic data processing, for example wave equation migration, use the Fast Fourier Transform (FFT) on a regular grid for computational efficiency. Irregular trace spacing, therefore, must be accounted for when FFT based processing is to be used.

As a demonstration, a simple spatial-domain processing procedure is illustrated, plus a Fourier-domain antialias filter is given as a demonstration in Figures 1 and 2. In Figures 1a, c, e and g respectively we have a spatial domain signal that corresponds to an input wave form, a sampling function that is evenly spaced, a sampling function applied to the input waveform, and a sinc function (antialias) applied to the sampled signal (aliased), resulting in antialiased signal.

In seismic acquisition, the continuous signal (Figure 1a) is multiplied (digitized) with a sampling function (Figure 1c). Energy in the spectrum of resulting signal (Figure 1f) is aliased beyond the Nyquist frequency of the sampling function (here, 40 Hz), as can be seen by comparing Figure 1b to Figure 1d. Antialiasing is achieved by multiplication of the aliased spectrum with the spectrum of a High cut filter (Figure 1b). The resulting spectrum (Figure 1j) is then returned to the time domain by the Inverse Fast Fourier Transform (IFFT). The total cost of this process is equivalent to the cost of the FFT plus the IFFT.

A similar processing flow is adopted in Figure 2, except that the sampling function

(Figure 2c) is irregular. The energy spectrum of the irregularly sampled signal (Figure 2f) is also aliased beyond the Nyquist frequency of the sampling function (here, 40 Hz), as can be seen by comparing Figures 2b and 2d. But along with aliasing, noise is observed (Figure 2f) in the spectrum with a peak at $x = 0$. The process of antialiasing fails to remove the aliasing and noise present in the spectrum, the resultant spectrum (Figure 2j) obtained by this process is different from the original one. Even the reconstructed signal obtained (Figure 2j) in a spatial-domain by application of IFFT is erroneous. Figure 1 and 2 show the failure of conventional processing methods in handling the irregularly sample data.

Several approaches can be found which are based on some kind of interpolation techniques, but most of these approaches do not handle the data optimally. Transformation methods which include Radon transformations have been used to handle the problem of irregular sampling (Ronen et al., 1991). In the parabolic Radon transform, two CMP gathers are combined to improve offset sampling, and thus differences between mid point positions are ignored (Duijndam et al., 1999). Similarly, hyperbolic and linear Radon transforms (Thorson and Clarebout, 1985) as well as the parabolic Radon transform are suitable for estimating frequencies at irregular nodes, but they suffer aliasing problems due to sparse sampling (Hugonnet and Canadas, 1995). Several other approaches are suggested by Kabir and Thorson (1995) and Kelamis et al. (1985) to make these transformations more efficient. Prediction error filtering (Claerbout, 1992; Spitz, 1991) is another method which is used to interpolate missing traces, but it works only on regularly sampled data, and it only corrects for aliasing. If sampling is irregular, the result will be erroneous. Ronen (1987) and Ronen et al. (1991) suggests a method for DMO stacks which can handle irregular sampling, but it is still not efficient for very large seismic data volumes. Approximate regularization/datuming (Ferguson, 2006) allows extrapolation of data recorded on an irregular grid onto a regular grid, but it requires a velocity model.

Other techniques are proposed which can be seen as a generalization for regularization (Dutt and Rokhlin, 1993; Beylkin, 1995; Dutt and Rokhlin, 1995; Steidl, 1997; Duijndam and Schonewille, 1999; Greengard and Lee, 2004; Lee and Greengard, 2005). These methods are approximation approaches which can be used with an FFT for non equispaced points, and can be alternatives for current methods applied in processing of irregular samples. These algorithms find an approximate solution efficiently.

Algorithms that handle irregular sampling do so in two steps, the forward problem and the inverse problem. The forward problem is used to obtain the approximate spectrum in the Fourier domain, the Inverse problem is used to reconstruct the signal back in the original domain. Generally, the forward problem has asymptotic complexity of $O(N^2)$, and the Inverse problem complexity depends upon the approach adopted for signal reconstruction. Speed is the bottle neck for both the forward process and inverse process.

My aim in this paper is to solve the forward case with a faster algorithm, as done by Duijndam and Schonewille (1999) and Greengard and Lee (2004). I will begin with the theory behind the algorithm structure for NFFT and NDFT. After reviewing the basic algorithms, improvements are suggested in the NFFT algorithm. Then, using synthetic examples, I compare FFT, NDFT, and NFFT, and I show that the NFFT is approximately 100 times faster than the NDFT, and that the approximate spectrum obtained using NFFT
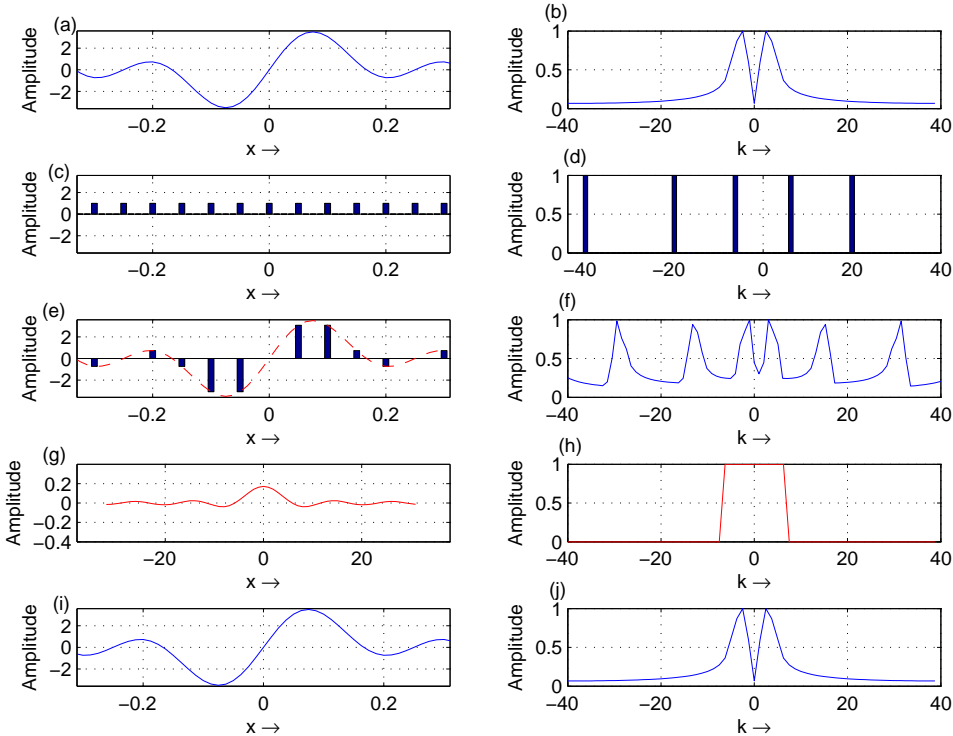
FIG. 1. (a) Original signal. (b) Fourier domain for Original signal. (c) Regular spaced sampling function. (d) Fourier domain (regular space) for sampling. (e) Sampled signal. (f) Aliased spectrum for sampled signal. (g) Sinc function. (h) Antialias Box car. (i) Reconstructed spatial domain. (j) Reconstructed Fourier domain.
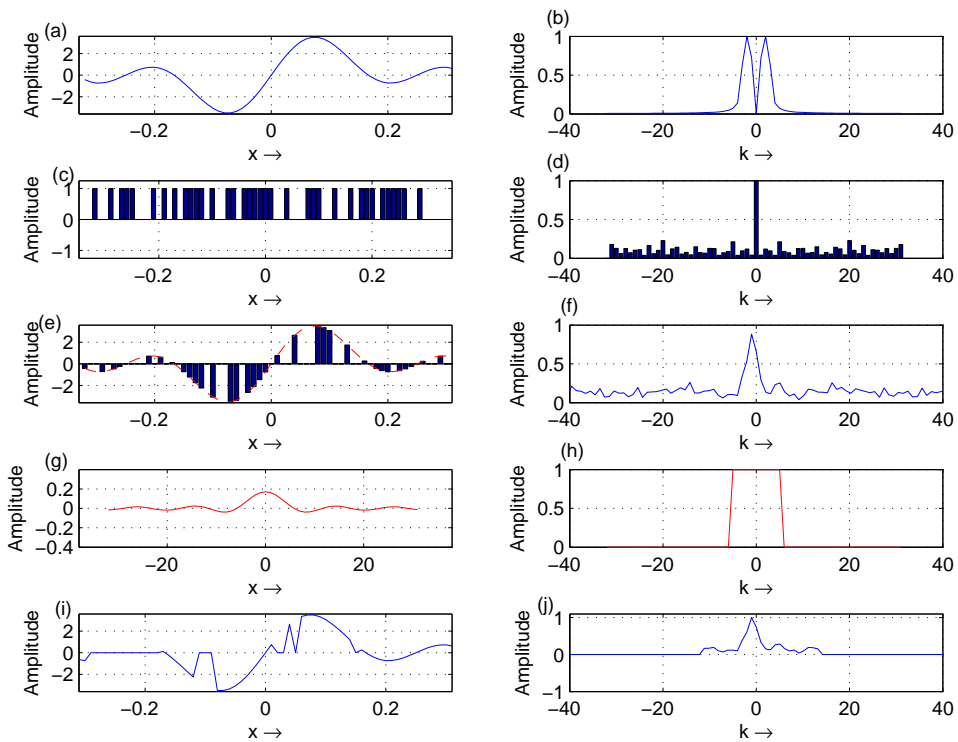
FIG. 2. (a) Original signal. (b) Fourier domain for Original signal. (c) Irregular spaced sampling function. (d) Fourier domain (irregular space) for sampling. (e) Sampled signal. (f) Aliased noisy spectrum for sampled signal. (g) Sinc function. (h) Antialias Box car. (i) Erroneously reconstructed spatial domain. (j) Erroneously reconstructed Fourier domain.

gives a good approximation to the original spectrum.

THEORY

When data are irregularly sampled, a straightforward discretization of the forward transformation corresponding to the irregular grid at hand will be highly erroneous. Instead, one can take the exact inverse transform from the regularly sampled domain to an irregularly sampled domain and use this as a forward model in an inverse problem. This is the basic approach for the hyperbolic Radon transform and the linear Radon transform by Thorson and Clarebout (1985). If desired, data estimated in the Fourier domain can be transform back to a regular grid in the spatial domain.

The forward discrete Fourier transform (DFT) for regularly sampled data can be given as

$$\hat{P}\left(k_x, \omega\right) = \Delta x \sum_{n=0}^{N-1} P\left(n\Delta x, \omega\right) e^{-ink\Delta x}, \tag{1}$$

where Δx is the sample interval in the spatial domain, k_x is the wave number, and ω is the temporal frequency. Periodicity is obtained in the Fourier domain due to regular sampling in the spatial domain.

In equation 1, Δx should be chosen small enough to avoid aliasing in the Fourier domain. DFT is the transformation of an N point signal $(x_1, x_2, \cdots x_N)$ into N Fourier coefficients X_K. In matrix vector form the DFT can be denoted as

$$X = Fx, \tag{2}$$

where F is the Fourier kernel. From equation 2, F is a matrix that maps an N dimensional vector x into another N dimensional vector X. To transform back to the spatial domain, we need F^{-1}. 'The inverse discrete Fourier transform is defined by

$$P\left(x, \omega\right) = \frac{\Delta k}{2\pi} \sum_{m=-M}^{m=M} \hat{P}\left(m\Delta k, \omega\right) e^{-im\Delta kx}, \tag{3}$$

where Δk is the sampling interval in the Fourier domain, $N = 2M + 1$, and $\Delta k = \frac{2\pi}{N\Delta x}$. The matrix vector form of equation 3 is

$$x = F^H X, \tag{4}$$

where F^H is the Hermitian transpose of F. Since sampling is regular, $F_{N\times N}$ is orthogonal so that.

$$F^H F = N I_N, \tag{5}$$

where I_N is the identity matrix. Equation 5 shows that a DFT is an orthogonal transformation, and that the inverse is computed using a Hermitian operator. The cost of inverting an $N \times N$ Hermitian operator is $O(N^2)$ instead of $O(N^3)$. Cost is greatly diminished using the fast Fourier transform (FFT) for matrix vector multiplication. FFT moreover can't be applied in the case of irregular sampling because an irregular Fourier matrix F is no longer
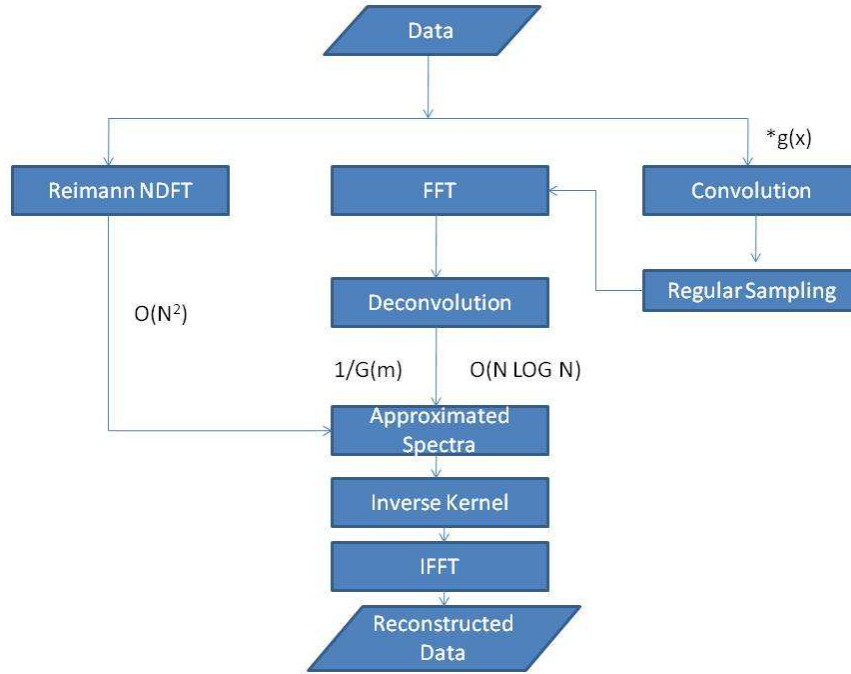
FIG. 3. Flow chart representation of the reconstruction Algorithm

orthogonal. A Riemann method is generally applied when sampling is irregular according to

$$P(m\Delta k, \omega) = \sum_{n=0}^{N-1} P(x_n, \omega)e^{jm\Delta k x_n}\Delta x_n, \tag{6}$$

where Δk is the regular sample interval in Fourier domain. x_n represents position of irregular nodes, and Δx_n is the irregular sampling interval which can be defined as

$$\Delta x_n = \frac{x_{n+1} - x_{n-1}}{2}, \quad n = 0, ..., N-1. \tag{7}$$

The transform in equation 6 can be referred to as a nonuniform discrete Fourier transform (NDFT). The NDFT, however, is not a unitary transformation, and it fails the dot product test (i.e. the dot product of two vectors before the transformation should be equal to the dot product after the transformation). For this reason, it is not possible to reconstruct the data in the original domain by a simple inverse FFT (IFFT). Figure 3 shows the algorithm structure of data reconstruction with NDFT as one of the major steps. The forward model approach has been suggested by Feichtinger and Grochenig (1993) and by Duijndam et al. (1999) to handle the problem of irregular sampling, where Δk is the sampling step size in the Fourier domain, and the data are band limited to between $[-M\Delta k, M\Delta k]$. Accordingly, equation 3 for N irregular samples in case of irregularly spaced sample locations$(x_0, x_1 \cdots, x_{N-1})$ can be denoted in matrix vector notation as

$$y = A\hat{p}, \tag{8}$$

where,

$$y_n = P(x_n, \omega), \tag{9}$$

$$\hat{p}_m = \hat{P}(m\Delta k, \omega), \tag{10}$$

and

$$A_{nm} = \frac{\Delta k}{2\pi}e^{-jm\Delta k x_n}. \tag{11}$$

In reality, data are never band limited, and some spatial frequency exist beyond the bandwidth. These unwanted frequencies can be characterized as noise in the forward model and can be included in equation 8 as

$$y = A\hat{p} + Noise \tag{12}$$

Equation 12 can be seen as a standard linear inverse problem where $\hat{p}$ is the unknown quantity. Data in the regularly sampled Fourier domain are to be estimated using the known quantity y, the irregularly sampled data in the spatial domain. A least squares estimate for $\hat{p}$ is proposed by Duijndam et al. (1999) according to

$$\hat{p} = \left(A^H W A + k^2 I\right)^{-1} A^H W y, \tag{13}$$

where W is a weight matrix, k is the stabilization factor, and A^H is the complex conjugate transpose of A. From equations 9, 10, and 11, the last term of equation 13 can be written as

$$A^H W y = \frac{\Delta k}{2\pi} \sum_{n=0}^{N-1} P(x_n, \omega)e^{jm\Delta k x_n}W_{nn}, \tag{14}$$

where $W_{nn} = \Delta x_n$. Here, except for the constant $\frac{\Delta k}{2\pi}$, equation 14 is equivalent to equation 6, which represents NDFT. So, $\hat{p}$, obtained after applying the inverse kernel, will give the correct spectrum, as shown in algorithm structure in Figure 3. The estimated Fourier spectrum $\hat{p}$ can be transformed back to the spatial domain by direct inverse transform. The NDFT is a bottle neck for the forward transform, as the computational complexity of the NDFT is $O(N^2)$. Many inversion schemes that are used in data processing (Sacchi and Ulrych, 1995, 1997; Duijndam et al., 1999; Hindirks et al., 1997) rely on the solution of normal equations, the right-hand side of which is an NDFT.

The NFFT is a solution that can replace a slow NDFT with a faster algorithm, thereby allowing the use of many schemes which hitherto ccould not be applied for practical purposes due to their high computational cost.

NFFT algorithms are based on the convolution of a sampled signal with a band limiting filter, and several different names are used in the literature. Jackson et al. (1991), and Pelt (1997) discuss these algorithms in terms of image processing and refer to them as griding algorithms. Beylkin (1995) proposes a similarscheme as the irregular Fourier transform algorithm where convolution with B-splines is carried out to make the signal approximately band limited. Jackson et al. (1991) discussed several forms of filters which can be used, and a truncated Gauss filter is introduced by Dutt and Rokhlin (1993).

Duijndam and Schonewille (1999) define an NFFT algorithm that consists of the convolution of a signal $p(x)$ with a short filter $g(x)$. This convolution maps $p(x)$ onto the regular grid, followed by fast Fourier transform (FFT). Deconvolution with an infinite length filter

in the Fourier domain corrects for convolution. NFFT is shown as a substitute for NDFT as in Figure 3. Two parameters are significant in our algorithm, one is the numerical width q of the truncated filter, the other is the analytical width b of the Gaussian filter.

The NFFT algorithm can be numerically expressed in the following steps: convolution, FFT, deconvolution. Convolution with the short Gaussian filter $g(x)$ is carried out to make the signal approximately band-limited according to

$$p_g(m) = g(x) * p(x), \tag{15}$$

where $p_g(m)$ is the result of a spatial convolution. Equation 15 can be written as a multiplication in the Fourier domain as

$$P_g(m) = G(m) \times P(m), \tag{16}$$

where $P_g(m)$ is the Fourier spectrum of $p_g(m)$. For efficiency, the Gaussian need to be truncated, thus generating n samples for $p_g(m)$ where

$$n = -int\left(\frac{q+1}{2}\right) + 1, \cdots, N + int\left(\frac{q+1}{2}\right) - 1, \tag{17}$$

and where $int(x)$ truncates to the largest integer smaller than x for $x \geq 0$. The algorithm is initialized at $p_{\tilde{g}}(n) = 0$, where the subscript $\tilde{g}$ indicates we apply a truncated Gaussian and keep updating by summation of the N shifted filters. This summation of N shifted filters can be given by

$$p_{\tilde{g}}(n) \leftarrow p_{\tilde{g}}(n) + \Delta x p_n g(n\Delta x - x_n) \tag{18}$$

Equation 18 spreads the irregular samples onto a regular grid. The sampling $p_{\tilde{g}}(n) = \Delta x p_1(n\Delta x)$ is similar to equation 19 in the Fourier domain which can be written as

$$P_g(m) = \sum_{I \in Z} P(m + IN)G(m + IN) \tag{19}$$

When $P_g(m)$ is broadband, aliasing will occur when $G(m + IN) \neq 0$ for any $I \neq 0$. It is suggested (Duijndam and Schonewille, 1999) that removal of the aliasing requires making the signal periodic.

$$p_{\tilde{g}}(n) = \sum_{I=-\infty}^{\infty} p_{\tilde{g}}(n + IN), \ \ n = 0, 1, 2, \cdots, N - 1, \tag{20}$$

where $p_{\tilde{g}}(n + lN) = 0$ outside the interval given by equation 17. Convolution of the signal followed by the discrete transform can be represented by

$$P_g(m)_{FFT} = \sum_{n=0}^{N-1} p_{\tilde{g}}(n)e^{j2\pi nm/N}, \ \ m = \frac{N}{2}, \cdots, \frac{N}{2} - 1 \tag{21}$$

where $P_g(m)_{FFT}$ is the spectrum obtained using the FFT. Finally correction for convolution is carried out by deconvolution in the Fourier domain according to

$$P(m) = \frac{P_g(m)_{FFT}}{G(m)}, \tag{22}$$

where $P(m)$ is the approximate spectrum and $G(m)$ has been defined by Dutt and Rokhlin (1993) as

$$G(m) = \sqrt{\frac{\pi}{b}} e^{\frac{m^2}{4b}} \quad m = -M/2 - 1 : M/2 - 1. \tag{23}$$

The spectrum obtained by equations 6 and 22 is an approximate spectrum; the direct inverse transformation (IFFT) cannot be applied using this approximate spectrum since the NDFT and NFFT are not unitary transformations. As shown in Figure 3, the inverse kernel needs to be applied to this approximate spectrum, followed by IFFT to reconstruct the signal. All available inversion schemes are expensive; hence, an attempt will be made to modify these inversion schemes with the application of Fast Multipole Methods (FMM) along with highly optimized Basic Linear Algebra Subprograms (BLAS) on the available inversion schemes.

Computation time

The Computational cost for the NDFT is $O(N^2)$ operations; N is the number of irregularly spaced samples. The computational cost of the NFFT is $NlogN$ as shown in table 1.

Table 1. Computational cost of NFFT algorithm

Step	Cost
Convolution	qN
FFT	$NlogN$
Deconvolution	N

The total time for the NFFT algorithm (Duijndam and Schonewille, 1999) can be written as

$$t = c_1 N \prod_{l=1}^{d} q_l + c_2 \prod_{l=1}^{d} N_l \sum_{l=1}^{d} logN_l + c_3 \prod_{l=1}^{d} N_l \tag{24}$$

where l specifies the dimension; the first term on the right-hand side represents the computational complexity of the convolution in the spatial domain; the second term represents the FFT which is usually of the form $NlogN$; term three is the window correction in the Fourier domain; and c_1, c_2, and c_3 are processor dependent constants.

Choosing parameters

Different types of filters were proposed in the literature (Dutt and Rokhlin, 1993; Beylkin, 1995; Dutt and Rokhlin, 1995; Steidl, 1997; Duijndam and Schonewille, 1999); the truncated Gauss filter by Duijndam and Schonewille (1999) was found to be optimal for this purpose. Both the numerical width q and the analytical width b affect the performance of the low pass filter. Increasing the numerical width of Gaussian increases the accuracy of the results. From equation 24 it is clear that increasing q will increase the computational cost. In Figure 4, the relative RMS error is calculated between the NDFT and the NFFT
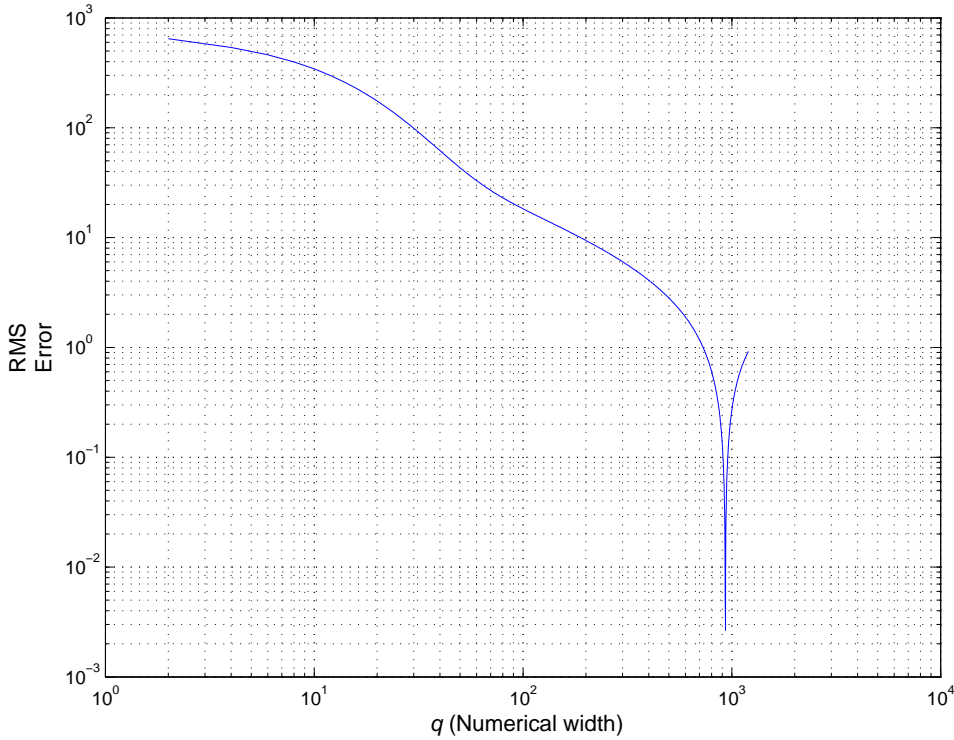
FIG. 4. RMS error between NDFT and NFFT output for a varying numerical width.

for different values of q.

$$RMS_{Error} = \frac{\sqrt{\sum_m |P(m) - P_4(m)|^2}}{\sum_m |P_m|^2} \tag{25}$$

In Figure 4, it is observed that for 2000 sample points the value of the error keeps on decreasing until a particular q is reached, and after that it starts increasing again. It is seen in many other papers that value of q is always kept such that $q \leq \frac{N}{2}$ (Dutt and Rokhlin, 1993; Beylkin, 1995; Dutt and Rokhlin, 1995; Steidl, 1997; Duijndam and Schonewille, 1999; Greengard and Lee, 2004; Lee and Greengard, 2005) which is again validating our algorithm. In Figure 5, an attempt is made to find the optimal value of b. It is observed that, for any signal the value of b differs, and that after an optimal value is reached the error will start increasing again. The numerical width of the Gaussian is another important parameter on which the performance of our algorithm depends. Different authors suggested different empirical expressions, but the value of b uses in theoretical expressions always differs from the experimental width, but can be used to define a nearby limit. According to Dutt and Rokhlin (1993)

$$b = \frac{\pi f^2 M^2}{q} \tag{26}$$

The value of b as defined by Duijndam and Schonewille (1999)

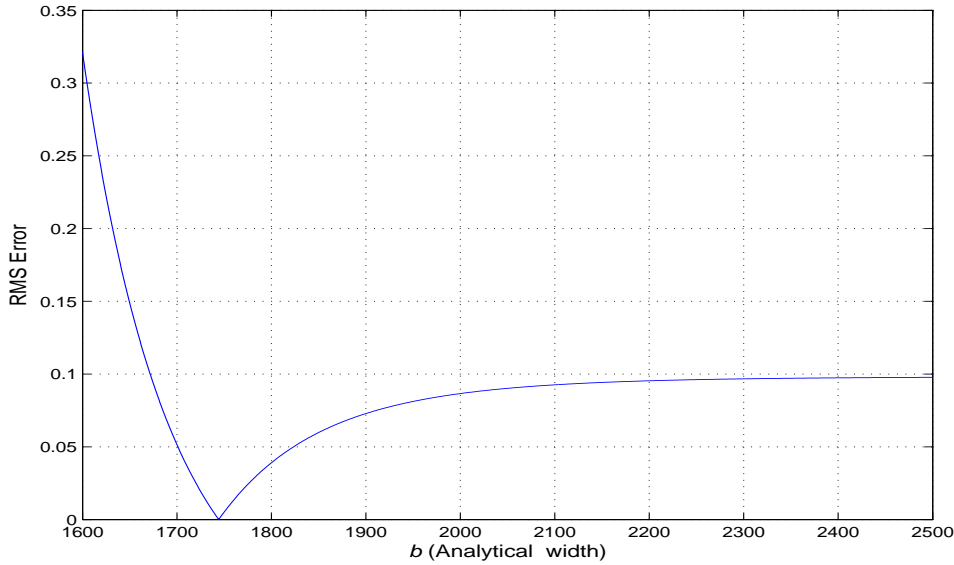$$b = \frac{\pi (2f^2 - f) M}{q} \tag{27}$$

FIG. 5. RMS error between NDFT and NFFT output for a varying analytical width.

In both of the above relations, f represents an oversampling factor which authors generally take as 2, but in our case no effect of an oversampling factor is seen. On the basis of numerical experiments, an improvement is suggested with respect to the width of the Gauss pulse. Empirically, an analytical Gaussian width can be written as

$$b = \frac{4.75}{q \times dx^2},$$ (28)

where dx is the spacing of regular grid.

EXAMPLES

In the example section, the NFFT is validated by applying it to a broad range of signals. As a first example, a Ricker wavelet is used as the input for the NFFT algorithm, than a comparison has been done using analytical, available solutions of Ricker wavelets. After this spectrum of a sine signal is evaluated using NFFT, the reason for using a sine is to check the algorithm on a simple signal. Following this is the application to a more complex signal in the form of a seismic trace. The only reason for taking different examples is to demonstrate the prove validity of the NFFT as a general algorithm for any irregularly sampled signal. In all these examples, results are compared with the original spectrum of the signal which is computed using an FFT on a regularly sampled signal, and with an analytical solution in the case of a Ricker wavelet. Algorithms cannot be applied, unless they are compared with some analytically available solution. For this purpose we are applying our algorithm to the analytically available solution of a Ricker wavelet. A Ricker wavelet has a very simple form in the time domain, it is given by

$$w(t)_{Ricker} = [1 - 2\pi^2 f_{dom}^2 t^2]e^{-\pi^2 f_{dom}^2 t^2}$$ (29)

which is also expressed as the second derivative of a Gaussian. In the above equation, f_{dom} is the dominant frequency of the wavelet. The frequency domain representation (Sheriff

and Geldart, 1995) of this can be written as

$$W(f) = \frac{2f^2}{\sqrt{(\pi)}f^2} e^{\frac{-f^2}{f_{dom}^2}} \tag{30}$$

Figure 6, shows an application of the NFFT on the uniformly sampled Ricker wavelet which is giving the same result in Figure 6(b) as the analytical solution in Figure 6(c) of the wavelet. It can be seen that the analytical solution in Figure 7(b) and FFT in Figure 7(c) on the non uniformly sampled Ricker wavelet as in Figure 7(a) are not similar, indicating the failure of the FFT in dealing with non uniform sampled wavelet. Figure 7(d) displays the Frequency spectrum of a non uniformly sampled wavelet, after applying NFFT on it. Figure 7(c) shows that we are not loosing any frequency points, there is loss of amplitude due to a lesser number of Fourier coefficients for processing. Figure 8(c) displays the effect of increasing the number of sample points, and makes it non-uniform. Increasing the number of sample points elevates the noise in the spectrum, although all frequencies are obtained. This presence of noise can be explained from the fact that in NFFT, columns of the Fourier matrix are not orthogonal to each other. Also, some noise will be observed when the signal is undersampled (Claerbout, 1992).
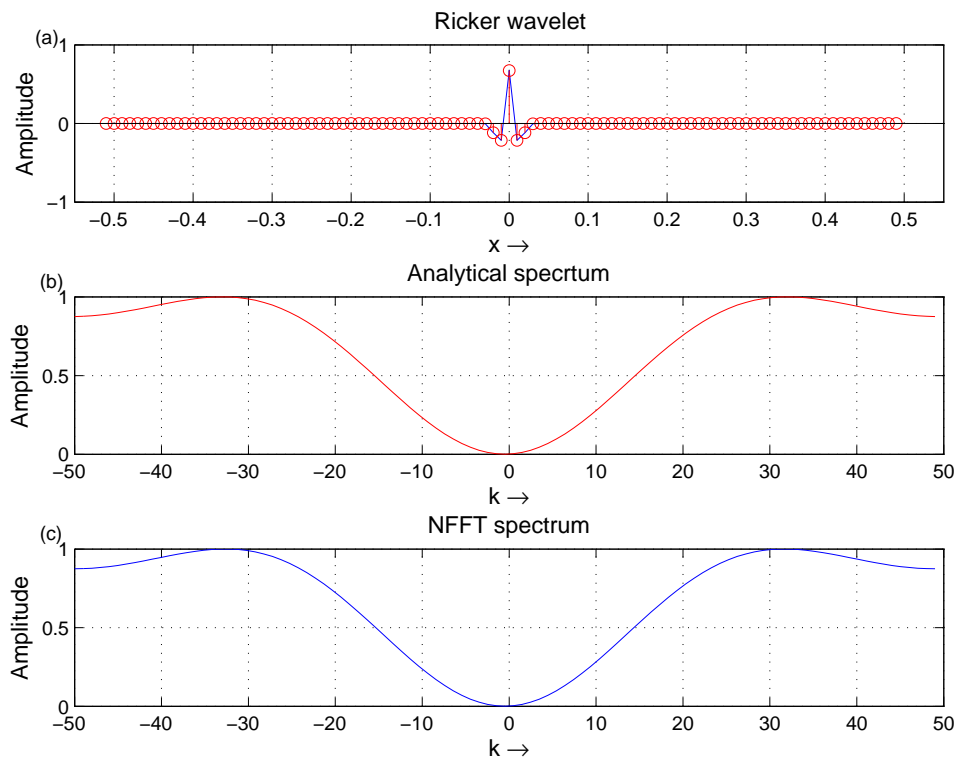

FIG. 6. Comparison of analytical and NFFT spectra of a uniformly sampled Ricker wavelet.
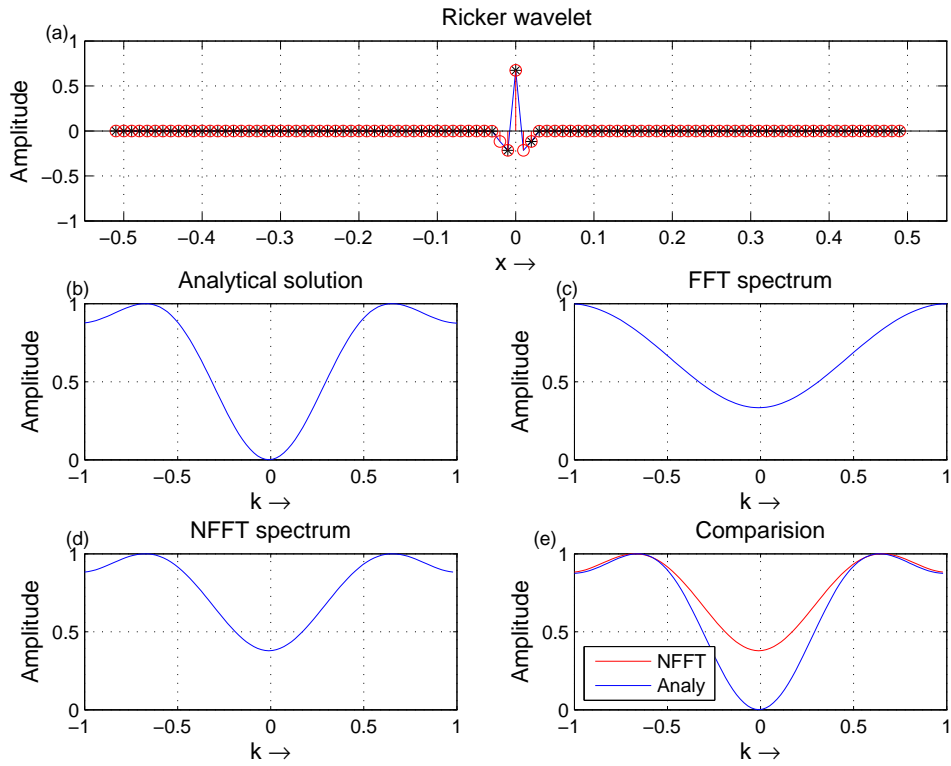
FIG. 7. Comparison of Analytical and NFFT spectra of a nonuniformly sampled Ricker wavelet.
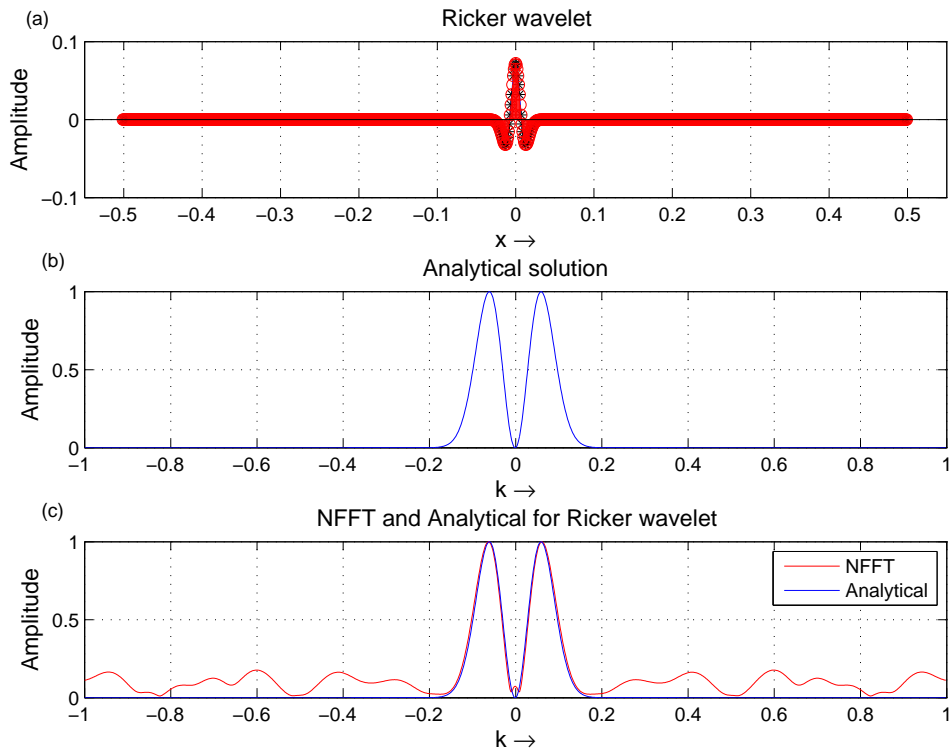

FIG. 8. Display of noise with a high number of samples.

It is important for any algorithm to be tested on different cases, therefore, two synthetic examples are taken. Figure (9) shows the sine signal which is irregularly sampled, missing Fourier coefficients can be seeare indicatedn. Figure (10) displays the NFFT and FFT spectrum, results are similar to what we observed in the case of validation. NFFT is able to compute the frequencies at the irregular node points. Similarly, Figure (11) shows a Seismic trace with 5000 sample points and 25 percent decimation. Higher analytical width is needed for seismic trace, as compared to a sine signal. It is observed from Figure (9) that NFFT is giving a good approximation of our problem. Most of the frequency points are there, none of them seem to be missing. It is clear from Figure (8) and Figure (12) that the number of samples increases the noise in the spectrum, distorting the spectrum. Noise will also be unavoidable in the presence of undersampling. A relative RMS error of the order of 10^{-1} with respect to the FFT of the original spectrum has been found in both the approximated spectrum of the seismic trace and the sine signal.
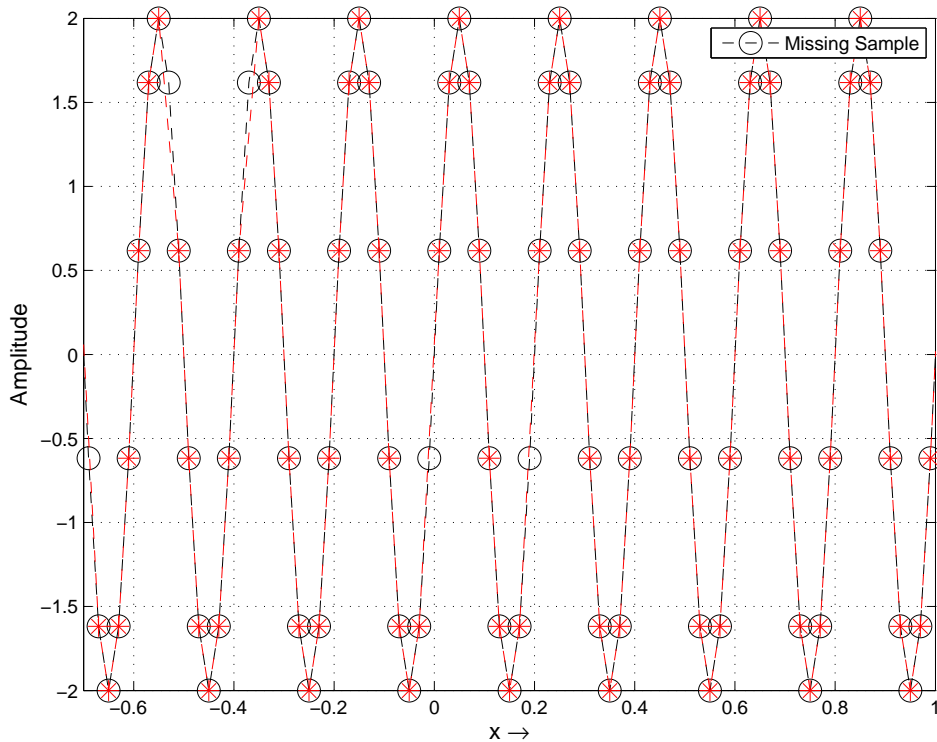

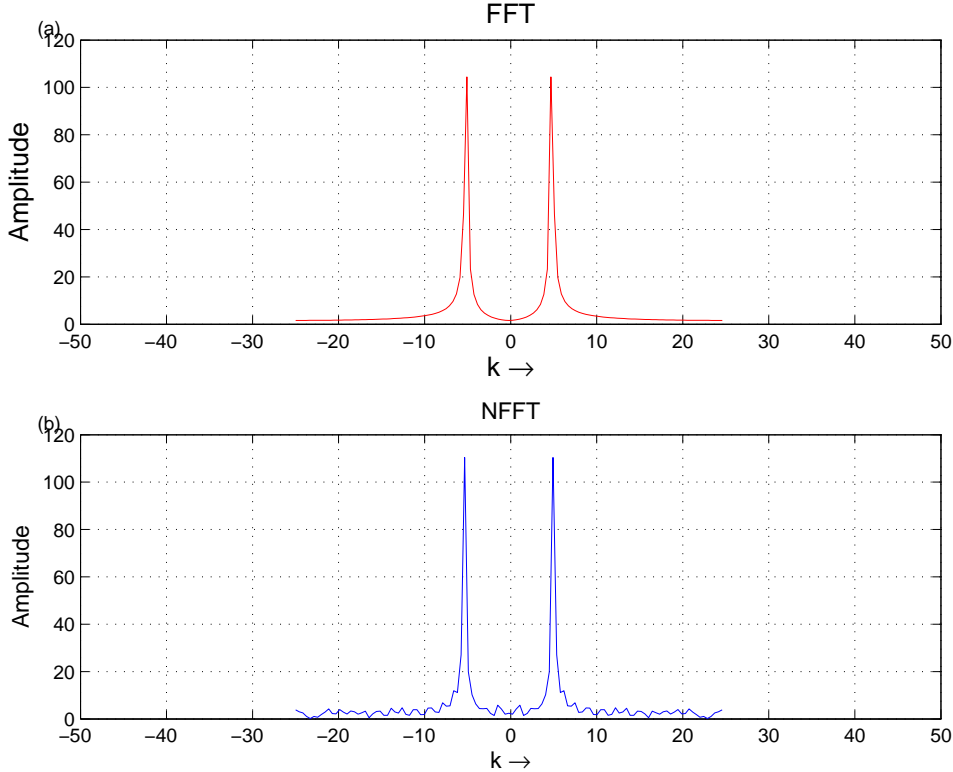FIG. 9. Non uniform sampled sine signal

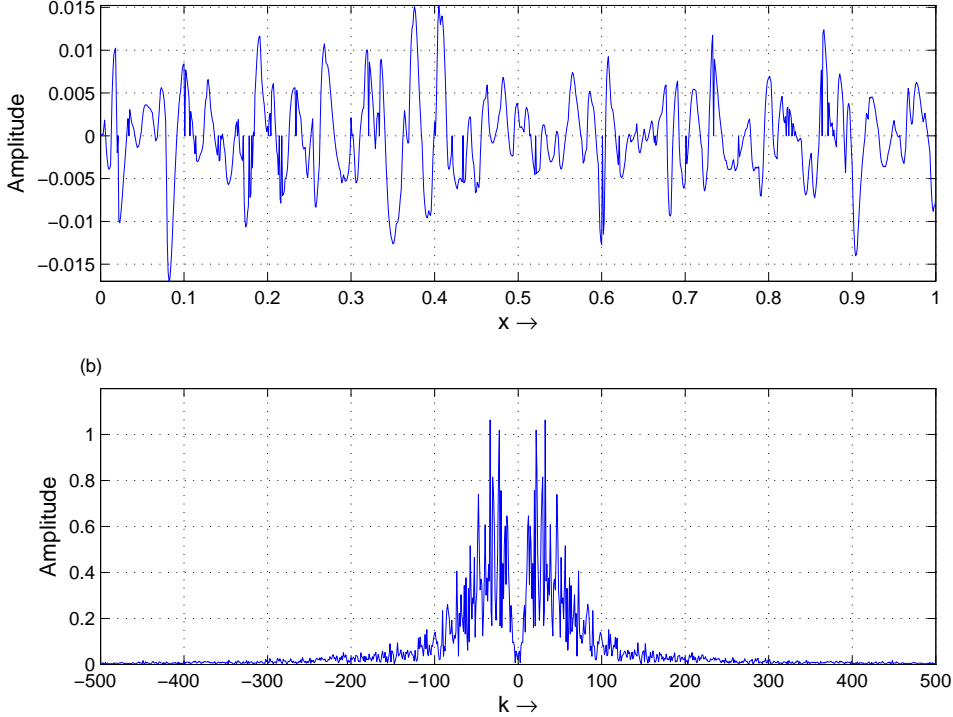FIG. 10. FFT and NFFT spectrum for an Non uniform sampled sine wave

FIG. 11. A Trace and its spectrum
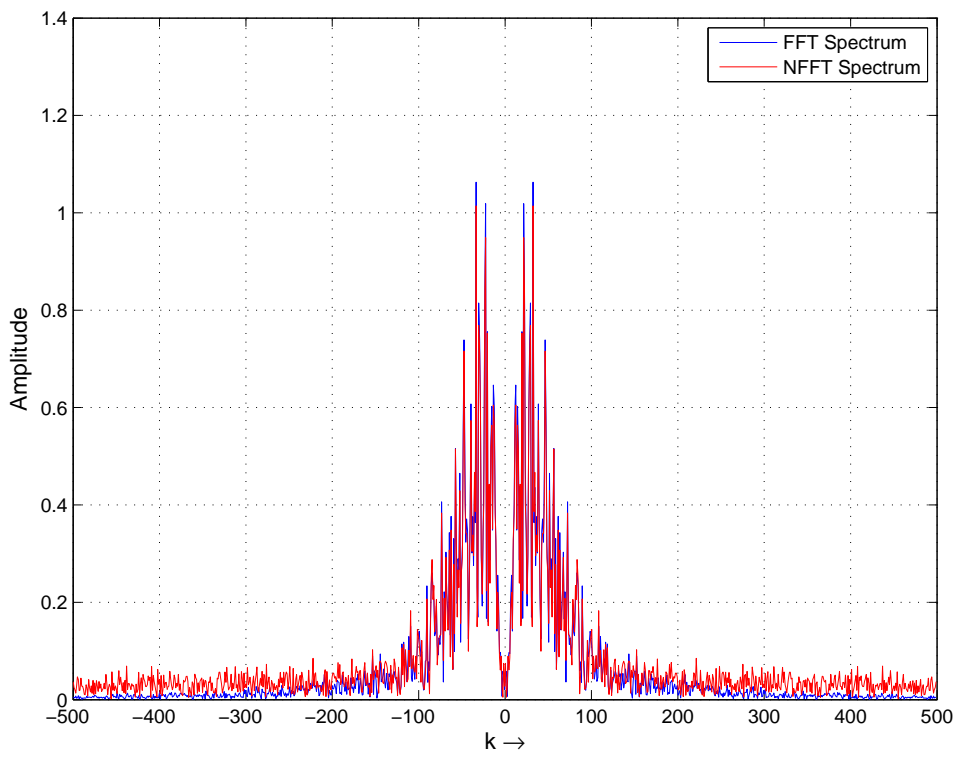
FIG. 12. Non uniform sampled trace

Efficiency of Algorithm

The Efficiency of any algorithm is measured by its accuracy and its speed. It is very important for an algorithm to be tested in both areas.

100	0.0078	5.4	15.
500	0.0102	29.63	24.2
1000	0.013	48.2	34.4
2000	0.16	195.5	51.2
5000	0.299	1125.	96.6
7000	0.407	2177.7	137.2
10000	0.645	4390.	190.5
15000	0.971	10020.	258.
20000	1.3	22197.	383.

Table 2 compare's the computational performance of three different algorithms: FFT, NDFT and NFFT, respectively. When the number of samples is around 100, the time requirement of NFFT exceeds that of NDFT. But as the number of sample increases, the time ratio of NDFT and NFFT becomes more due to increasing time requirement of NDFT with an increase in the number of sample points.

100	1.2E-04	1.63E-05
500	1.5E-04	1.7E-05
1000	1.7E-03	2.0E-05
2000	1.8E-03	2.2E-05
5000	2.2E-03	8.7E-04
7000	2.0E-03	7.9E-04

Table 3 gives the Error analysis of algorithms. The Error measured here is the Relative mean square error with respect to FFT or the original spectrum. The errors increase with the number of samples. But they are small as needed in many practical purposes.

DISCUSSION AND CONCLUSION

NFFT can be a major part of conventional algorithms. The tremendous improvement over NDFT allows us to handle large impractical and uneconomical data sets in an efficient way. Performance of our algorithm depends upon the type of low cut filter used and the analytical width of the filter plays a major role in the algorithm. NFFT can be used in place of other slow methods like the Riemann sum method, which have been used in the past to process irregular sampled signal. A new generation of fast algorithms can be developed based on the NFFT approach, which can take advantage of irregular sampling to handle the problem of aliasing.

FUTURE WORK

The NFFT approach is a solution of a forward problem. When the reconstruction of a signal is needed, the inverse approach is adopted for solving the problem. Numerous methods exist in literature for inversion. All of them are very slow and computationally inefficient. Attempts will be made to modify the existing methods to solve the inverse problem by introducing recently developed algorithms known as "Fast Multipole Methods". An FMM is a way to accelerate the product of particular dense matrices with vectors, using $O(N)$ memory instead of $O(N^2)$ memory. Combined with iterative solution methods like conjugate gradient, this can allow the solution of problems hitherto unsolvable. My aim in this project is to develop fast algorithms which can be used for the practical purpose of seismic data processing. The peak performance of these algorithms later will be calculated on refined model's of BLAS (Basic Linear Algebra subroutines) like GOTO BLAS. GOTO BLAS works on the high performance implementation of matrix multiplication.

REFERENCES

Beylkin, G., 1995, On the fast fourier transform of function with singularities: Appl. Comp. Harmon, **2**, 363–381.

Claerbout, J., 1992, EARTH SOUNDINGS ANALYSIS: Processing versus Inversion (PVI): Cambridge University Press.

Duijndam, A. J. W., and Schonewille, M. A., 1999, Nonuniform fast fourier transform: Geophysics, **64**, 551–573.

Duijndam, A. J. W., Schonewille, M. A., and Hindriks, C. O. H., 1999, Reconstruction of band-limited signals, irregularly sampled along one spatial direction: Geophysics, **64**, 542–538.

Dutt, A., and Rokhlin, V., 1993, Fast fourier transforms for nonequispaced data: SIAM J. Sci. Comput., **14**, 1368–1393.

Dutt, A., and Rokhlin, V., 1995, Fast fourier transforms for nonequispaced data: Appl. Comput. Harmon. Anal, 85–100.

Feichtinger, H. G., and Grochenig, K., 1993, Theory and practice of irregular sampling: In Benedetto, J. and Frazier, M., editors, Wavelets: Mathematics and Applications, 305–363.

Ferguson, R. J., 2006, Regularization and datuming of seismic data by weighted, damped least square: Geophysics, **71**, 67–76.

Greengard, L., and Lee, J.-Y., 2004, Accelerating the non uniform fast fourier transform: SIAM Review., **46**, 443–454.

Hindirks, C. O. H., Duijndam, A. J. W., and Petersen, S., 1997, Reconstruction of ban-dlimited data, irregularly sampled along two spatial directions: 59th EAGE Conference, **Extended Abstracts**, A033.

Hugonnet, P., and Canadas, G., 1995, Aliasing in the parabolic radon transform: 65th Annual Internat. Mtg. Soc. Expl. Geophy., Expanded Abstracts, **95**, 1366–1369.

Jackson, I. J., Meyer, C. H., Nishimura, D. G., and Macovsky, A., 1991, Selection of convolution function for fourier inversion usning gridding: IEEE Trans Med. Imag., **14**, 471–478.

Kabir, M. M. N., and Thorson, D. J. V., 1995, Restoration of missing offset by parabolic radon transform: Geophysics Prospecting, **43**, 347–368.

Kelamis, P. G., Chiburis, E. F., and Shahryar, S., 1985, Radon multiple elimination, a practical methodology for land data: In 60th Annual Internatioal Mtg. Soc. Expl. Geophy Expanded Abstracts, **90**, 1611–1613.

Lee, J.-Y., and Greengard, L., 2005, The type 3 nonuniform fft and its applications: J. Comput. Phys., **206**, 1–5.

Pelt, J., 1997, Fast computation of trigonometric sums with application to frequency analysis of astronomical data: Proc. Florence and Georgewise observatory 25th Aniv. Symp., 179–182.

Ronen, J., 1987, Wave equation trace interpolation: Geophysics, **52**, 973–984.

Ronen, J., Sorin, V., and Bale, R., 1991, Spatial dealiasing of 3-d seismic reflection: Geophy. J. Int, **105**, 503–511.

Sacchi, M. D., and Ulrych, T. J., 1995, High resolution velocity gathers and offset space reconstruction: Geophysics, **60**, 1169.

Sacchi, M. D., and Ulrych, T. J., 1997, Estimation of the discrete fourier transform, a linear inversion approach: Geophysics, **1122**.

Sheriff, R. E., and Geldart, L. P., 1995, Exploration Seismology: Cambridge University Press.

Spitz, S., 1991, Sesimic trace interpolation in the f-x domain: Geophysics, **56**, 785–794.

Steidl, G., 1997, A note on fast fourier transforms for nonequispaced grids: Adv. Comp. Math.

Thorson, J. R., and Clarebout, J. F., 1985, Velocity-stack and slant stack stochastic inversion: Geophysics, **50**, 2727–2741.

Zwartjes, P. W., and Sacchi, M. D., 2007, Fourier reconstruction of nonuniformly sampled, aliased seismic data: Geophysics, **72**.